Published OnlineFirst January 12, 2010; DOI: 10.1158/0008-5472.CAN-09-2501

Integrated Systems and Technologies: Mathematical Oncology

Cancer Research

Predicting Outcomes in Cervical Cancer: A Kinetic Model of Tumor Regression during Radiation Therapy

Zhibin Huang[1], Nina A. Mayr[1], William T.C. Yuh[2], Simon S. Lo[1], Joseph F. Montebello[1], John C. Grecula[1], Lanchun Lu[1], Kaile Li[1], Hualin Zhang[1], Nilendu Gupta[1], and Jian Z. Wang[1]

Abstract

Applications of mathematical modeling can improve outcome predictions of cancer therapy. Here we present a kinetic model incorporating effects of radiosensitivity, tumor repopulation, and dead-cell resolving on the analysis of tumor volume regression data of 80 cervical cancer patients (stages 1B2-IVA) who underwent radiation therapy. Regression rates and derived model parameters correlated significantly with clinical outcome ($P < 0.001$; median follow-up: 6.2 years). The 6-year local tumor control rate was 87% versus 54% using radiosensitivity (2-Gy surviving fraction $S_2 < 0.70$ vs. $S_2 \geq 0.70$) as a predictor ($P = 0.001$) and 89% vs. 57% using dead-cell resolving time ($T_{1/2} < 22$ days versus $T_{1/2} \geq 22$ days, $P < 0.001$). The 6-year disease-specific survival was 73% versus 41% with $S_2 < 0.70$ versus $S_2 \geq 0.70$ ($P = 0.025$), and 87% vs. 52% with $T_{1/2} < 22$ days versus $T_{1/2} \geq 22$ days ($P = 0.002$). Our approach illustrates the promise of volume-based tumor response modeling to improve early outcome predictions that can be used to enable personalized adaptive therapy. *Cancer Res; 70(2); 463–70. ©2010 AACR.*

Major Findings

A kinetic model was developed to predict the ultimate clinical outcome of radiation therapy (RT) for cervical cancer. Tumor volume regression assessed by serial magnetic resonance imaging before, during, and after RT was linked to radiobiological parameters, which reflect the underlying biological processes of cellular response to RT. This study suggests that patient-specific modeling of tumor growth kinetics can provide valuable information on biological mechanisms of tumor radioresponse and predict long-term clinical outcome.

Introduction

Despite the best standard-of-care treatment, radiation/chemotherapy is unsuccessful in one third of all patients with cervical cancer. Prognostic indicators of treatment outcome have traditionally been derived from clinical and pathologic features, including the Fesddration Internationale des Gynaecologistes et Obstetristes stage, lymph node status, primary tumor size, and histology. Tumor size is an important prognostic factor for local control (LC) and survival in cervical cancer (1–4), but its assessment by clinical palpation has been relatively inaccurate. Magnetic resonance imaging (MRI) has been reported to be much more precise than any other modality in delineating uterine tumors (1, 5–8). It has been previously shown that the important prognostic factor of tumor volume can be measured more precisely using three-dimensional MRI-based volumetry (6, 9) and tumor regression rate can be accurately evaluated by sequential MRI obtained before, during, and after the course of radiation therapy (RT; refs. 1, 5).

Tumor volume regression rate has also been suggested as an important predictor of LC and long-term survival (1, 10, 11), which can provide essential information about the inherent response of cervical cancer to the cytotoxic radiation/chemotherapy regimen. To date the intrinsic tumor radiobiological factors influencing tumor regression are largely unknown in cervical cancer. Therefore translation of tumor regression information into clinical decision-making for individualized adaptive therapy has not been possible. A better understanding of these radiobiological processes and establishment of robust modeling parameters would refine the accuracy of outcome prediction and may enable biological-based optimization of therapy.

In 2006, we first developed a kinetic model (12) to analyze MRI-based tumor regression data in cervical cancer. The radiobiological model incorporated three major effects of RT: radiation cell-killing, tumor repopulation, and dead/inactivated cell resolving. In this pilot study, we found that tumor regression rate and radiobiological modeling strongly correlated with treatment outcome (12, 13). In 2008, Lim and colleagues (14) developed a similar model describing tumor regression during external beam RT (EBRT); they found that the model parameters correlated with tumor hypoxia. However, no outcome correlation was available.

Authors' Affiliations: Departments of [1]Radiation Medicine and [2]Radiology, The Ohio State University, Columbus, Ohio

Corresponding Author: Jian Z. Wang, Department of Radiation Medicine, James Cancer Hospital and Solove Research Institute, The Ohio State University, 300 West 10th Avenue, Room 094, Columbus, OH 43210. Phone: 614-293-6502; Fax: 614-293-4044; E-mail: wang.993@osu.edu.

doi: 10.1158/0008-5472.CAN-09-2501

Published OnlineFirst January 12, 2010; DOI: 10.1158/0008-5472.CAN-09-2501

Quick Guide: Main Model Equations

Eq. (A):

$$\begin{cases} \dfrac{dR(t)}{dt} = & -\dfrac{\ln 2}{T_{1/2}}[R(t)-S(t)], \\ \dfrac{dS(t)}{dt} = & S(t)\left[-(1-S_2)+\dfrac{\ln 2}{T_d}\right]. \end{cases}$$

This is a differential equation used to describe the tumor volume regression profile $R(t)$, in terms of three major radiobiological processes: radiation cell-killing, dead-cell resolving, and tumor repopulation. The equation relates the temporal regression rate $R(t)$ of tumor volume at time t, with the half-time of dead-cell resolving $T_{1/2}$ and the cell surviving fraction at time t, $S(t)$, which is ultimately related to the basic radiobiological parameters: cell surviving fraction after 2-Gy (S_2) and effective tumor doubling time (T_d).

Major Assumptions of the Model:

This model assumes that the tumor volume regression during radiation therapy (RT) is determined by three major biological processes: radiation cell-killing implied by radiosensitivity S_2, the clearance of tumor dead cells with a half-time $T_{1/2}$, and tumor cell repopulation with a doubling time T_d. First, tumor cells are killed/inactivated by RT; then the damaged clonogenic cells lose their reproductivity but remain *in situ* where they die and eventually are cleared by blood circulation, reticuloendothelial system, or surface sloughing. Therefore, we did not anticipate an immediate change of tumor volume after each RT fraction. Rather, we assumed that the second process, resolving of dead cells, would follow in an exponential fashion. As more and more tumor cells were killed and cleared, the blood and nutrient supply to the tumor would improve. Then, the third process, repopulation of the living clonogens, would begin.

Long-term clinical follow-up data is necessary to verify the usefulness of kinetic modeling parameters for outcome prediction (13).

The purpose of our study was to present the details of the kinetic model and to analyze the tumor regression data using the kinetic model and estimate tumor radiosensitivity and dead-cell resolving time for individual patients. These radiobiological parameters were correlated to therapy outcome to assess their value for outcome prediction and their potential for individualized RT.

Materials and Methods

Patient population. Among a total of 115 patients with carcinoma of the cervix accrued prospectively in this study, 80 patients completed all four serial MRI scans. The patients were staged clinically by International Federation of Gynecology and Obstetrics criteria (15), including physical examinations, chest radiograph, tumor biopsy, complete blood count, serum chemistries, intravenous pyelogram, and abdomino-pelvic computed tomography. There were 10 patients in Stage IB, 5 in Stage IIA, 26 in Stage IIB, 3 in Stage IIIA, 24 in Stage IIIB, 7 in Stage IVA, 2 in Stage IVB (inguinal metastasis), and 2 with locally recurrent tumors (after hysterectomy). Sixty-nine patients had squamous cell, and 11 had adenocarcinomas. Median age was 55 y (range, 25–89).

Standard RT. All patients were treated with primary RT with curative intent, which included a combination of pelvic EBRT with 24 MV photons (45–50 Gy delivered in daily 1.8–2.0 Gy fractions) and low-dose rate (LDR) intracavitary brachytherapy. The brachytherapy consisted of one to two fractions of 20 Gy prescribed to Point A, which was converted to equivalent EBRT doses of 18 Gy using an α/β of 10 Gy (16). Twenty-six patients received cisplatin-based chemotherapy.

In this study, data analysis focused on two outcome end points, tumor local failure (LF) and dead of disease, based on clinical follow-up. LF was defined as tumor recurrence during the follow-up period or persistent/progressive tumor within pelvis. Cases other than LF were considered as LC of tumor. For dead of disease, death from cervical cancer or cancer complications was scored as event and death from intercurrent disease was censored. Patients other than dead of disease were considered as disease-specific survival (DSS).

MRI protocol and tumor volume measurement. Serial MRIs were performed for each patient at four time points: at the start of RT, during RT (at 20–25 and 40–45 Gy of pelvic RT), and at follow-up (1–2 mo after RT). The 320 MRI scans were obtained with 1.5-Tesla superconductive scanners (Signa, General Electric Medical Systems and Siemens Magnetom Vision, Siemens Medical, Inc.) in all but five patients who were imaged with a 0.5-Tesla scanner (Picker International) in the early phase of this study. Imaging included sagittal 5-mm conventional fast spin, echo T_2-weighed images (TE_{eff} = 104, TR = 4,000, ETL = 10, NEX = 2), and axial 7-mm T_2-weighed and T_1-weighed images (TE = 16, TR = 600, NEX = 2).

Published OnlineFirst January 12, 2010; DOI: 10.1158/0008-5472.CAN-09-2501

Tumor region-of-interest (ROI) was delineated in each slice on T_2-weighed images, and three-dimensional ROI-based tumor volumes were calculated using a technique described previously (5). The tumor regression rate was determined for each measurement as the percentage of residual tumor volume at a given time normalized to the initial tumor volume.

Kinetic regression model. A kinetic model was developed to describe tumor regression during RT and to analyze the tumor volume data.

During the RT course, three major processes were considered relevant to tumor response (12). First, tumor cells are killed/inactivated by RT; then the damaged clonogenic cells lose their reproductivity but remain *in situ* where they die and are eventually cleared by the blood circulation, reticulo-endothelial system, or surface sloughing. Therefore, we did not anticipate an immediate change of tumor volume after each RT fraction. Rather, we assumed that the second process, resolving of dead cells, would follow in an exponential fashion. As more and more tumor cells were killed and cleared, the blood and nutrient supply to the tumor would improve. Then, the third process, repopulation of the living clonogens, would begin (17). Therefore, the tumor regression profile $R(t)$ can be described by Eq. (A) (12). The onset time of tumor repopulation is assumed to be T_k. The T_k data for cervical cancer are very scarce in the literature; therefore, in this study, we tested two cases with T_k = 0 and T_k = 21 d as found in the published data for other types of human cancer (17, 18).

Numerical calculation method. Because of the complex dose delivery schedule, including both EBRT and LDR brachytherapy, and weekend and unscheduled breaks, it was unpractical to derive an analytic solution for Eq. (A). Therefore, a numerical method of iteration was adopted to derive the regression profile $R(t)$ for each individual patient. To mimic the clinical conditions, actual dose delivery schedules were extracted from the RT charts for all 80 patients and taken as input parameters of our model calculation.

$$D_i = \begin{cases} 0 & i \text{ represents a day without radiation;} \\ 1.8 \text{ or } 2.0 \text{ Gy} & i \text{ represents a day with EBRT;} \\ D_{LDR} & i \text{ represents a day with LDR brachytherapy.} \end{cases}$$

Here index i represents the ith day during the course of RT, starting at 1 when the first daily fraction of EBRT was delivered. Dose D_{LDR} represents the actual dose of Point A normalized to EBRT dose in 1.8-Gy fractions.

Assuming that the initial tumor volume is V_0 and V_i represents the volume on ith day, here V_i consists of two partial volumes $V_{s,i}$ and $V_{d,i}$: $V_{s,i}$ represents the volume made up of living clonogenic cells and $V_{d,i}$ is the volume composed of the inactivated/dead cells, i.e.,

$$V_i = V_{s,i} + V_{d,i}, \qquad (B)$$

and the relative tumor volume on the ith day is given by

$$R_i = V_i/V_0. \qquad (C)$$

Early investigations by Bentzen and colleagues (19) showed that the tumor volume is directly proportional to the clonogen number. Therefore, the tumor volume change during radiotherapy with dose data (D_i, i = 1,...,n) can be calculated as follows,

$$V_{s,i} = \begin{cases} V_{s,i-1}S_2^{n_i}, & \text{when } i \le T_k, \\ V_{s,i-1}S_2^{n_i} + V_{s,i-1}e^{\ln 2/T_d}, & \text{when } i > T_k, \end{cases}$$

$$V_{d,i} = V_{d,i-1}e^{\ln 2/T_{1/2}}, \qquad (D)$$

where $V_{s,i-1}$ and $V_{d,i-1}$ stand for the volumes of clonogens and inactivated cells on the (i–1)th day, respectively and n_i equals 1 for RT days and 0 for non-RT days. When i = 0, $V_{s,0} = V_0$ and $V_{d,0}$ = 0.

S_2 and $T_{1/2}$ for patient groups and individual patients. We simulated the tumor regression based on the kinetic model for each patient during the RT course. Radiobiological parameters were derived by fitting the tumor regression data. Four model parameters were evaluated in the data analyses, including S_2, $T_{1/2}$, T_d, and T_k. Because we had only four data points for each patient, and one of them was the normalization point, we had to reduce the model parameters in our fitting exercises. Among the four parameters, tumor regression profile was most sensitively influenced by S_2 and $T_{1/2}$; therefore, only S_2 and $T_{1/2}$ were treated as free parameters. Lim and colleagues (14) suggested that the possible values within reasonable physiologic ranges are 0.01 to 0.99 for S_2 and 1 to 100 d for $T_{1/2}$. Data for tumor doubling time (T_d) of cervical cancer published in the literature gave median values ranging from 3.1 to 5.6 d (20–25). An average value of 4.5 d was adopted in our model. The onset time (T_k) of tumor repopulation plays a role in tumor regression during RT and was assumed to be 0 or 21 d (16, 17, 26).

The tumor volumes measured by the four MRIs were included as the input data for the modeling study. The initial tumor volume was obtained from the first MRI, and all subsequent volumes were normalized to this initial value to obtain the tumor regression ratios at the designed time points. When the initial MRI preceded the start of RT, the tumor volume was assumed to be constant (assuming tumor cell proliferation and cell loss were balanced) before the start of treatment. For the few cases in which the initial MRI scan was several days later than the start of RT, the parametric volume at the beginning of treatment was assumed to be 1, and the tumor volume corresponding to the date of the first MRI was calculated using the above method of iteration; once all volume data were obtained, they were renormalized to this calculated volume of the initial MRI.

The tumor regression data were also summarized and analyzed for two outcome groups: LC versus LF. The mean tumor volumes corresponding to the four sequential MRIs were obtained and then normalized to the mean initial tumor volume. The time points of the four MRI scans were adopted as

Published OnlineFirst January 12, 2010; DOI: 10.1158/0008-5472.CAN-09-2501

Table 1. The means and the ranges of tumor volume and regression ratio measured by the four MRI scans

Patient outcome group	Patient no.	MRI scans	Mean volume, cm^3 (volume range)	Mean regression ratio, %
LC	62	1	66.3 (3.0–342.0)	100
		2	36.3 (0.4–248.4)	50.3
		3	8.4 (0.0–48.1)	12.4
		4	0.6 (0.0–13.0)	0.6
LF	18	1	129.5 (41.0–700.0)	100
		2	96.2 (20.2–492.8)	76.9
		3	46.7 (1.9–191.8)	39.0
		4	26.2 (0.0–121.0)	19.4

0, 16, 36, and 100 d after RT started. Dose data were taken as input parameters in the model fits but were simplified by using the standard treatment regimen/schedule.

Statistical analyses for outcome prediction. In the current study, we analyzed the S_2 and $T_{1/2}$ data for different outcome groups and tested the significance of their differences. Furthermore, we derived the model parameters for each individual patient and correlated them with the ultimate outcome.

In this study, the model fitting of tumor profiles was performed with in-house c++ code. All statistical analyses were performed on the SPSS (SPSS 16, SPSS, Inc.). Correlations between the model parameters and the clinical outcome were assessed by either the Mann-Whitney rank sum test or Pearson correlation. Receiver operating characteristics (ROC) analysis was adopted to select optimal model classifiers. Survival curves were obtained using Kaplan-Meier survival analysis. Using the Cox regression method, multivariate analysis incorporating stage, lymph node status, initial tumor volume, S_2, and $T_{1/2}$ was performed to verify independent prognostic factors for outcome prediction.

Results

Tumor regression profile. Tumor volume measurements were performed in 80 patients who had completed four serial MRI scans before, during, and after the RT course for cervical cancer by identifying and delineating the area of tumor based on MRI T2-weighed images. As an example, the regions of interest (tumor delineation) of a typical patient are shown in Fig. 1 for all four MRI studies. The tumor volume at the start of RT ranged from 3.4 to 700 cm^3 (median, 54.4 cm^3; Table 1) and had only marginal value for outcome prediction ($P = 0.06$). During EBRT, tumor regression occurred in all cases, following an exponential pattern, and the relative volume reduction and the shapes of the regression curves varied considerably during and at the end of treatment. Typical regression curves are shown in Fig. 2 for two patients with LC versus LF. Tumor regression profiles were calculated for each patient to best fit the regression data.

Modeling two outcome groups: LC versus LF. The radiobiological parameters of S_2 and $T_{1/2}$ were obtained by fitting the mean tumor regression data to the two outcome groups shown in Table 1. The resulting parameters were $S_2 = 0.66$, $T_{1/2} = 9.5$ days for LC and $S_2 = 0.72$, $T_{1/2} = 18$ days for LF. The SD of S_2 and $T_{1/2}$ derived from the mean regression data were (0.26, 0.68) and (6.0, 17) days, respectively, for LC group and (0.22, 0.73) and (11, 31) days, respectively, for LF group. Differences between the LC and LF groups were statistically significant ($P = 0.015$ for S_2 and $P = 0.001$ for $T_{1/2}$).

Evaluation of S_2 and $T_{1/2}$ for individual patients. Parameters S_2 and $T_{1/2}$ were derived by fitting the model to the

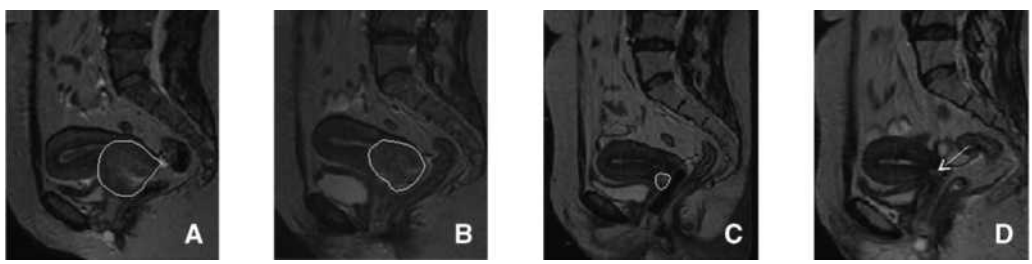

Figure 1. The contoured area of tumor based on T2-weighed images (*A*) before, (*B*) at 23.4 Gy, (*C*) at 45 Gy during RT, and (*D*) after the RT course, in a patient with stage IIB cervical cancer. Note that at 45 Gy (*C*), minimal tumor at <5% remains, and after completion of the RT course, no tumor is visible. *D, arrow,* the original site of the tumor.

Published OnlineFirst January 12, 2010; DOI: 10.1158/0008-5472.CAN-09-2501

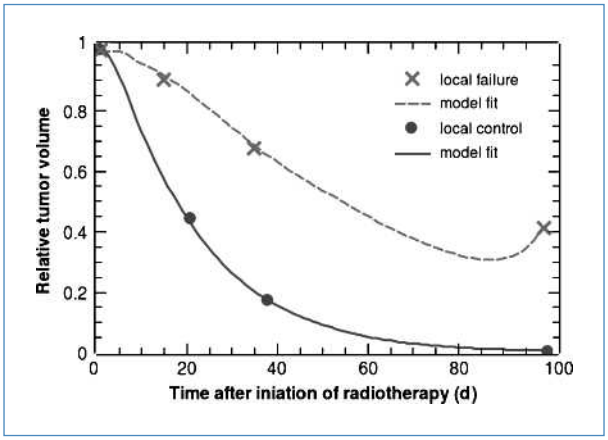

Figure 2. Typical tumor regression profiles: one patient from the LC group (*solid circles*) and another patient from the LF group (*crosses*). Dashed line and dash-dotted line represent the model fits of the data for the two patients, respectively. The model parameters S_2 and $T_{1/2}$ derived from fitting clinical data were 0.50 and 5.1 d, respectively, for the LC patient and 0.78 and 27 d, respectively, for the LF patient.

four tumor volumes of each of the 80 patients. Both S_2 and $T_{1/2}$ influenced the shape of the tumor volume regression profile during RT, as shown in Fig. 2. In general, a low S_2 and a short $T_{1/2}$ correlated with fast tumor regression. Relatively small S_2 values ($S_2 < 0.2$) were associated with a relatively large uncertainty. Therefore we chose a low boundary of S_2 to achieve a stable model fit. The fitting always yielded a unique value of $T_{1/2}$ with a relatively small uncertainty for individual tumors. S_2 and $T_{1/2}$ did not significantly correlate with each other ($P = 0.17$), whereas S_2 and $T_{1/2}$ were independently correlated with LC and DSS. Table 2 summarizes the fitting results of the two outcome categories with $S_2 = 0.65$ (median) and $T_{1/2} = 7.9$ days (median) for the LC tumors and $S_2 = 0.70$ (median) and $T_{1/2} = 18$ days (median) for LF tumors.

Outcome prediction with model parameters. The radiobiological parameters of S_2 and $T_{1/2}$ derived from the model were correlated with the clinical outcome. With $T_k = 21$ days, both S_2 and $T_{1/2}$ were significantly and independently correlated with treatment outcome ($P = 0.002$ and $P < 0.001$, respectively). With $T_k = 0$, the results were similar but with less significant P values ($P = 0.057$ and $P = 0.002$, respectively). The optimal cut-points for S_2 and $T_{1/2}$, based on the ROC analyses for outcome prediction, were $S_2 = 0.70$ and $T_{1/2} = 22$ days.

Kaplan-Meier analyses showed strong correlation of S_2 and $T_{1/2}$ with local tumor control (LC). Patients with $S_2 < 0.70$ had a 6-year LC rate of 87%, compared with 54% for higher S_2 values ($P = 0.001$; Fig. 3*A*). Similarly, the 6-year LC rate was 95% versus 57% for $T_{1/2} < 22$ versus $T_{1/2} \geq 22$ days ($P < 0.001$; Fig. 3*B*). The two model parameters also correlated strongly with DSS. As shown in Fig. 4*A*, patients with $S_2 < 0.70$ had a 6-year DSS rate of 73%, compared with 41% for those with $S_2 \geq 0.70$ ($P = 0.025$), and it was 87% versus 52% for $T_{1/2} < 22$ versus $T_{1/2} \geq 22$ days ($P = 0.002$; Fig. 4*B*).

Multivariate analysis for independent prognostic factors. In the multivariate analysis incorporating stage, lymph node status, initial tumor volume, S_2, and $T_{1/2}$, the results showed that the $T_{1/2}$, S_2, and initial tumor volume remained significant in outcome prediction ($P < 0.05$) and $T_{1/2}$ was the best predictive factor ($P < 0.001$); however, the classic prognostic parameters, including stage and lymph node status, were no longer significant ($P > 0.05$) in the multivariate analysis.

Discussion

Radiobiological modeling of tumor regression during RT enables us to estimate the intrinsic biological determinants for individual tumor response and interpret interpatient variability of tumor regression based on fundamental biological processes associated with radiosensitivity (S_2), time of dead-cell resolving ($T_{1/2}$), and accelerated repopulation of surviving colonogens (T_d and T_k).

To our knowledge, our study is the first report on early response modeling for outcome prediction in a large cervical cancer population with long-term clinical follow-up. Our model parameters, derived from the three-dimensional volumetric tumor regression analysis with direct outcome correlation, enabled us to classify tumors as radiosensitive or radioresistant to RT according to S_2 and perhaps as well or poorly perfused according to $T_{1/2}$. The results have shown that S_2 and $T_{1/2}$ can provide outcome prediction within a few weeks of treatment completion, in stark contrast to the currently available methods that do not allow determination of treatment success or failure until many months/years after therapy. The model-based early determination of a high risk of local tumor recurrence allows more aggressive therapy interventions to improve outcome for patients with cervical cancer.

Radiation sensitivity. Intrinsic cellular radiosensitivity and the repair capacity of radiation-damaged cells contribute to clinical radioresponsiveness. These characteristics also vary among tumors and depend on multiple factors, including differential sensitivity to induction of apoptosis and complex molecular mechanisms that are poorly understood. It has been shown that S_2 is one of the most significant prognostic

Table 2. The model parameters derived from tumor regression profiles of individual patients

Patient group	Patient no.	Model parameters	Median	Range
LC	62	S_2	0.65	0.20–0.75
		$T_{1/2}$ (d)	7.9	1.5–29
LF	18	S_2	0.70	0.20–0.85
		$T_{1/2}$ (d)	18	1.5–64

Published OnlineFirst January 12, 2010; DOI: 10.1158/0008-5472.CAN-09-2501

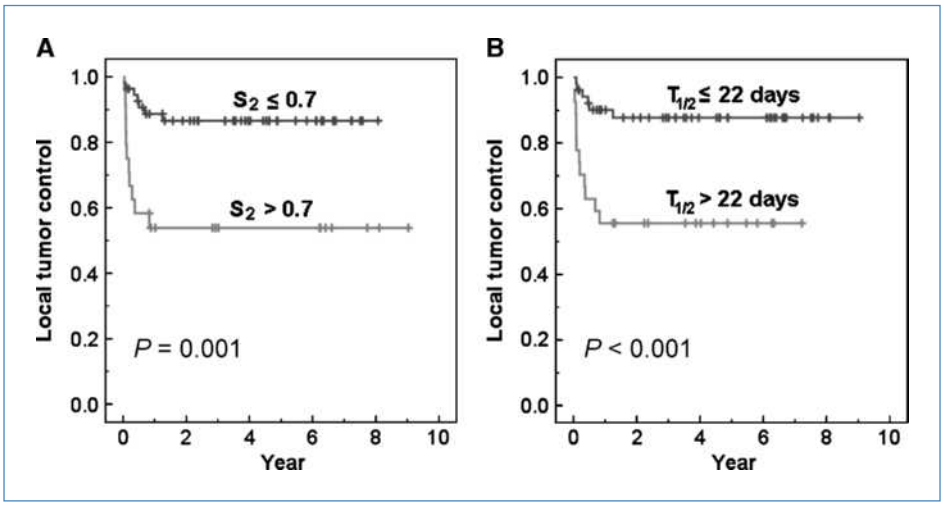

Figure 3. Kaplan-Meier survival analyses of local tumor control data using (*A*) radiosensitivity S_2 cut of 0.70 and (*B*) resolving half-time of inactivated cells $T_{1/2}$ cut of 22 d as outcome predictors.

factors for stage I to stage III cervical carcinoma treated with RT (27). Although surviving fraction analysis of tumor biopsies has a relatively high failure rate (28), the combination of S_2 with either apoptosis index (25) or tumor vascularity (29) improves the discrimination of the prognostic groups. Moreover, a Poisson tumor-control-probability model involving individual radiosensitivity has been found to be a better independent prognostic factor for LC and DSS in cervical cancer (30).

In our study, the delineation of radiosensitivity was directly derived from tumor response to ongoing therapy. Fitting the model to the patient clinical data enabled us to evaluate radiosensitivity in individual patients. Differences in S_2 were directly reflected in the different tumor volume regression patterns. Radiosensitive tumors with low S_2 were characterized by rapid tumor regression during RT; radioresistant tumors (high S_2) showed slow regression early in treatment (Fig. 2). The strong outcome correlation of S_2 suggests that the S_2 values derived in our analysis are robust in characterizing radiosensitivity-based tumor control in cervical cancer.

Lim and colleagues (14) found that the median $S_2 = 0.71$ could be used to classify patients with radiosensitive or radioresistant tumors and that tumors with S_2 higher than 0.71 were more hypoxic and radioresistant. Our outcome study was consistent with their result, with the optimal cutoff point of $S_2 = 0.70$ for radiosentivity classification, as found in the ROC analysis.

Dead-cell resolving. The half-time of dead-cell resolving ($T_{1/2}$) in our model is likely related to tumor microenvironment, including stromal components and vasculature. Although cell death in fractionated radiotherapy of carcinomas is dominated by mitotic catastrophe (31), it is still not clear how RT-induced cell death in highly complex and dynamic solid tumor systems translates into volume regression during/after RT. It has been suggested that radiation-induced impairment of blood flow reduces the dead-cell resolving rate (32). This concept is seemingly supported by observations of prolonged tumor regression caused by radiation-induced stromal cell damage (33). Thus, it is possible that tumors with more extracellular stroma might regress slowly, resulting in a

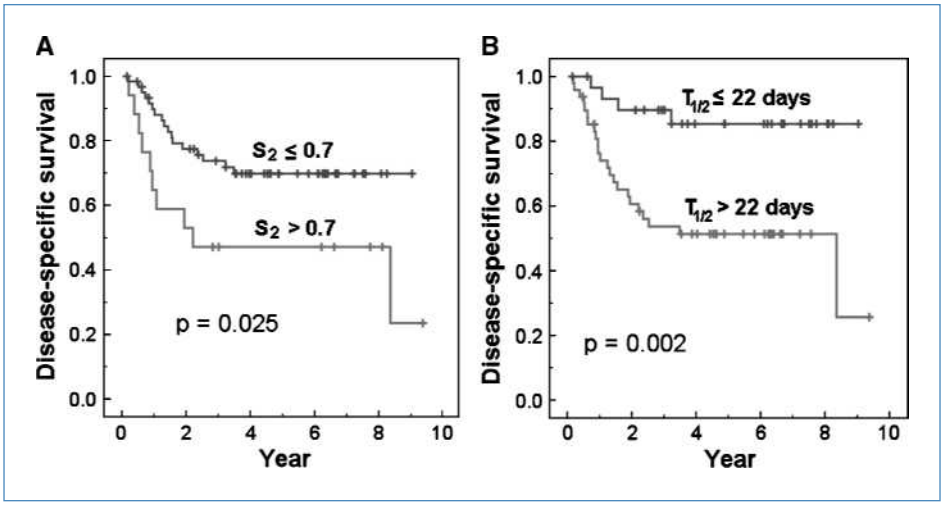

Figure 4. Kaplan-Meier survival analyses of disease-specific survival data using (*A*) radiosensitivity $S_2 = 0.70$ and (*B*) resolving half-time of inactivated cells $T_{1/2} = 22$ d as outcome predictors, respectively.

longer $T_{1/2}$. On the other hand, the dead-cell resolving is related to multiple biological processes influencing cell metabolism and death. Tumors are highly dynamic systems, including complex interactions among the cellular, stromal, and vascular compartments, mediated by cell-cell communication and physiochemical reactions associated with hypoxia, acidosis, and interstitial fluid pressure. Heterogeneous blood perfusion was observed in tumors using DCE-MRI technique, and variation in blood perfusion may occur within a short time interval (34). Whereas well-perfused tumors may have a short $T_{1/2}$, they would also have better blood supply and, thus, be well oxygenated, which may lead to more effective RT and better outcome. Therefore in our study, we found a strong inverse correlation between $T_{1/2}$ and tumor control.

Relationship between S_2 and $T_{1/2}$. Overall no significant correlation between S_2 and $T_{1/2}$ was found ($P = 0.17$, Pearson correlation). However, we observed that tumors with high S_2 regressed slowly in early RT and tended to be accompanied by a long $T_{1/2}$. A plausible explanation for this observation could be that both high S_2 and long $T_{1/2}$ could lead to slow tumor regression, and detailed profile data (more than four measurements for each patient) are necessary to differentiate the two biological processes. However, our outcome study indicates that the optimal cutoffs of S_2 and $T_{1/2}$ obtained from ROC analyses were powerful discriminators of the LC versus LF groups.

Tumor repopulation. Repopulation of surviving tumor clonogens during fractionated RT is one of the crucial factors determining radiocurability (22). In theory, pretherapy tumor proliferation is balanced by tumor cell loss due to apoptosis, necrosis, and sloughing, whereas the potential doubling time measures the potential growth of the tumor, assuming no cell loss (20, 35). Although there was a significant trend for patients with increasing tumor stage to have more rapidly proliferating tumors with a shorter T_d (21), results obtained by Hill and colleagues (21) showed that both tumor proliferation (shown by labeling index) and potential doubling time lost significance in predicting clinical outcome.

Many investigators have studied potential doubling time in cervical cancer (20–25). For instance, Bolger and colleagues (23) obtained a median potential doubling time of 4.0 days for cervical cancer, and Tsang and colleagues (36) found it to be 5.6 days. We used 4.5 days for our kinetic regression model, an average from these published data (20–25), as the effective tumor doubling time after repopulation start (T_d). In our previous model study analysis, using the mean value of $T_d = 3.5$ days reported by Wigg (25), S_2 and $T_{1/2}$ were 0.61 and 9.9 days for LC and 0.66 and 20 days for LF groups, respectively (12). Although in our current analysis, using a T_d of 4.5 days, S_2 and $T_{1/2}$ varied slightly (see Results), our data consistently showed that high S_2 and large $T_{1/2}$ are associated with unfavorable treatment outcome. More data and further study are necessary to evaluate the effect of tumor repopulation on clinical outcome for individual patients.

Although the model was applied to cervical cancer in this study, it can be suitable for other types of cancers, such as lung cancer, etc. The radiobiological parameters resulting from the kinetic model provide predictive value for clinical outcome. Due to limited image data, only four MRI scans were available during the RT course; our model had to focus on the major effects that influence the tumor regression significantly and was not able to address the underlying mechanism in detail, which is related to the fundamental radiation biology of human cancer.

In summary, a kinetic model was developed to describe the tumor regression of cervical cancer during radiotherapy. The model fits the temporal three-dimensional volume data well, as measured by serial MRI, and derives radiobiological parameters of radiosensitivity and dead-cell resolving halftime for individual patients. These model parameters correlate with clinical outcome significantly. The radiobiological modeling reflects the underlying biological and molecular processes influencing radiosensitivity and treatment outcome; therefore, this process has the potential to translate the tumor phenomenal response into treatment strategies for better therapy outcome.

Disclosure of Potential Conflicts of Interest

No potential conflicts of interest were disclosed.

Acknowledgments

We thank David Carpenter for editorial assistance.

Grant Support

NIH R01 CA 71906.

The costs of publication of this article were defrayed in part by the payment of page charges. This article must therefore be hereby marked *advertisement* in accordance with 18 U.S.C. Section 1734 solely to indicate this fact.

Received 7/27/09; revised 10/23/09; accepted 11/12/09; published OnlineFirst 1/12/10.

References

1. Mayr NA, Magnotta VA, Ehrhardt JC, et al. Usefulness of tumor volumetry by magnetic resonance imaging in assessing response to radiation therapy in carcinoma of the uterine cervix. Int J Radiat Oncol Biol Phys 1996;35:915–24.
2. Eifel PJ, Morris M, Wharton JT, Oswald MJ. The influence of tumor size and morphology on the outcome of patients with FIGO stage IB squamous cell carcinoma of the uterine cervix. Int J Radiat Oncol Biol Phys 1994;29:9–16.
3. Mendenhall WM, Thar TL, Bova FJ, et al. Prognostic and treatment factors affecting pelvic control of Stage IB and IIA-B carcinoma of the intact uterine cervix treated with radiation therapy alone. Cancer 1984;53:2649–54.
4. Perez CA, Grigsby PW, Nene SM, et al. Effect of tumor size on the prognosis of carcinoma of the uterine cervix treated with irradiation alone. Cancer 1992;69:2796–806.
5. Mayr NA, Taoka T, Yuh WT, et al. Method and timing of tumor volume measurement for outcome prediction in cervical cancer using magnetic resonance imaging. Int J Radiat Oncol Biol Phys 2002;52:14–22.

Published OnlineFirst January 12, 2010; DOI: 10.1158/0008-5472.CAN-09-2501

6. Burghardt E, Hofmann HM, Ebner F, et al. Magnetic resonance imaging in cervical cancer: a basis for objective classification. Gynecol Oncol 1989;33:61–7.
7. Sironi S, Belloni C, Taccagni GL, DelMaschio A. Carcinoma of the cervix: value of MR imaging in detecting parametrial involvement. AJR Am J Roentgenol 1991;156:753–6.
8. Hricak H, Quivey JM, Campos Z, et al. Carcinoma of the cervix: predictive value of clinical and magnetic resonance (MR) imaging assessment of prognostic factors. Int J Radiat Oncol Biol Phys 1993;27:791–801.
9. Greco A, Mason P, Leung AW, et al. Staging of carcinoma of the uterine cervix: MRI-surgical correlation. Clin Radiol 1989;40:401–5.
10. Mayr NA, Yuh WT, Zheng J, et al. Tumor size evaluated by pelvic examination compared with 3-D quantitative analysis in the prediction of outcome for cervical cancer. Int J Radiat Oncol Biol Phys 1997;39:395–404.
11. Mayr NA, Wang JZ, Lo SS, et al. Translating response during therapy into ultimate treatment outcome: a personalized 4-dimensional MRI tumor volumetric regression approach in cervical cancer. Int J Radiat Oncol Biol Phys 2009, (accepted).
12. Wang JZ, Mayr NA, Yuh WT, et al. Kinetic model of tumor regression during radiation therapy of cervical cancer. Int J Radiat Oncol Biol Phys 2006;66:S603.
13. Wang JZ, Mayr NA, Zhang D, Yuh WT. MRI for cervical cancer not only correlates with tumor hypoxia, but also predicts ultimate outcome: in regard to Lim et al. (letter). Int J Radiat Oncol Biol Phys 2008;71:1602–3;author reply 3.
14. Lim K, Chan P, Dinniwell R, et al. Cervical cancer regression measured using weekly magnetic resonance imaging during fractionated radiotherapy: radiobiologic modeling and correlation with tumor hypoxia. Int J Radiat Oncol Biol Phys 2008;70:126–33.
15. Annual report of treatment in gynecologic cancer. Int Fed Gynecol Obstet 1988;20:40.
16. Wang JZ, Li XA. Evaluation of external beam radiotherapy and brachytherapy for localized prostate cancer using equivalent uniform dose. Med Phys 2003;30:34–40.
17. Wang JZ, Guerrero M, Li XA. Low α/β ratio for prostate cancer: in response to Dr. Fowler et al. Int J Radiat Oncol Biol Phys 2003;57:595–6.
18. Withers HR, Taylor JM, Maciejewski B. The hazard of accelerated tumor clonogen repopulation during radiotherapy. Acta Oncol 1988;27:131–46.
19. Bentzen SM, Thames HD. Tumor volume and local control probability: clinical data and radiobiological interpretations. Int J Radiat Oncol Biol Phys 1996;36:247–51.
20. Symonds P, Bolger B, Hole D, Mao JH, Cooke T. Advanced-stage cervix cancer: rapid tumour growth rather than late diagnosis. Br J Cancer 2000;83:566–8.
21. Hill RP, Fyles W, Milosevic M, Pintilie M, Tsang RW. Is there a relationship between repopulation and hypoxia/reoxygenation? Results from human carcinoma of the cervix. Int J Radiat Biol 2003;79:487–94.
22. Trott KR, Kummermehr J. What is known about tumour proliferation rates to choose between accelerated fractionation or hyperfractionation? Radiother Oncol 1985;3:1–9.
23. Bolger BS, Symonds RP, Stanton PD, et al. Prediction of radiotherapy response of cervical carcinoma through measurement of proliferation rate. Br J Cancer 1996;74:1223–6.
24. Tsang RW, Juvet S, Pintilie M, et al. Pretreatment proliferation parameters do not add predictive power to clinical factors in cervical cancer treated with definitive radiation therapy. Clin Cancer Res 2003;9:4387–95.
25. Wigg DR. Applied radiobiology and bioeffect planning. Madison, Wisconsin: Medical Physics Publishing; 2001.
26. Roberts SA, Hendry JH. The delay before onset of accelerated tumour cell repopulation during radiotherapy: a direct maximum-likelihood analysis of a collection of worldwide tumour-control data. Radiother Oncol 1993;29:69–74.
27. West CM, Davidson SE, Roberts SA, Hunter RD. The independence of intrinsic radiosensitivity as a prognostic factor for patient response to radiotherapy of carcinoma of the cervix. Br J Cancer 1997;76:1184–90.
28. Moneef MA, Sherwood BT, Bowman KJ, et al. Measurements using the alkaline comet assay predict bladder cancer cell radiosensitivity. Br J Cancer 2003;89:2271–6.
29. Cooper RA, West CM, Wilks DP, et al. Tumour vascularity is a significant prognostic factor for cervix carcinoma treated with radiotherapy: independence from tumour radiosensitivity. Br J Cancer 1999;81:354–8.
30. Buffa FM, Davidson SE, Hunter RD, Nahum AE, West CM. Incorporating biologic measurements (SF(2), CFE) into a tumor control probability model increases their prognostic significance: a study in cervical carcinoma treated with radiation therapy. Int J Radiat Oncol Biol Phys 2001;50:1113–22.
31. Brown JM, Attardi LD. The role of apoptosis in cancer development and treatment response. Nat Rev Cancer 2005;5:231–7.
32. Bataini JP, Bernier J, Jaulerry C, et al. Impact of neck node radioresponsiveness on the regional control probability in patients with oropharynx and pharyngolarynx cancers managed by definitive radiotherapy. Int J Radiat Oncol Biol Phys 1987;13:817–24.
33. Budach W, Taghian A, Freeman J, Gioioso D, Suit HD. Impact of stromal sensitivity on radiation response of tumors. J Natl Cancer Inst 1993;85:988–93.
34. Brurberg KG, Benjaminsen IC, Dorum LM, Rofstad EK. Fluctuations in tumor blood perfusion assessed by dynamic contrast-enhanced MRI. Magn Reson Med 2007;58:473–81.
35. Steel GG. Growth kinetics of tumors. Oxford: Clarendon Press; 1977.
36. Tsang RW, Fyles AW, Li Y, et al. Tumor proliferation and apoptosis in human uterine cervix carcinoma I: correlations between variables. Radiother Oncol 1999;50:85–92.

Cancer Research

Correction: Online Publication Dates for *Cancer Research* April 15, 2010 Articles

The following articles in the April 15, 2010 issue of *Cancer Research* were published with an online publication date of April 6, 2010 listed, but were actually published online on April 13, 2010:

Garmy-Susini B, Avraamides CJ, Schmid MC, Foubert P, Ellies LG, Barnes L, Feral C, Papayannopoulou T, Lowy A, Blair SL, Cheresh D, Ginsberg M, Varner JA. Integrin $\alpha4\beta1$ signaling is required for lymphangiogenesis and tumor metastasis. Cancer Res 2010;70:3042–51. Published OnlineFirst April 13, 2010. doi:10.1158/0008-5472.CAN-09-3761.

Vincent J, Mignot G, Chalmin F, Ladoire S, Bruchard M, Chevriaux A, Martin F, Apetoh L, Rébé C, Ghiringhelli F. 5-Fluorouracil selectively kills tumor-associated myeloid-derived suppressor cells resulting in enhanced T cell-dependent antitumor immunity. Cancer Res 2010;70:3052–61. Published OnlineFirst April 13, 2010. doi:10.1158/0008-5472.CAN-09-3690.

Nagasaka T, Rhees J, Kloor M, Gebert J, Naomoto Y, Boland CR, Goel A. Somatic hypermethylation of *MSH2* is a frequent event in Lynch syndrome colorectal cancers. Cancer Res 2010;70:3098–108. Published OnlineFirst April 13, 2010. doi:10.1158/0008-5472.CAN-09-3290.

He X, Ota T, Liu P, Su C, Chien J, Shridhar V. Downregulation of HtrA1 promotes resistance to anoikis and peritoneal dissemination of ovarian cancer cells. Cancer Res 2010;70:3109–18. Published OnlineFirst April 13, 2010. doi:10.1158/0008-5472.CAN-09-3557.

Fiorentino M, Judson G, Penney K, Flavin R, Stark J, Fiore C, Fall K, Martin N, Ma J, Sinnott J, Giovannucci E, Stampfer M, Sesso HD, Kantoff PW, Finn S, Loda M, Mucci L. Immunohistochemical expression of BRCA1 and lethal prostate cancer. Cancer Res 2010;70:3136–9. Published OnlineFirst April 13, 2010. doi:10.1158/0008-5472.CAN-09-4100.

Veronese A, Lupini L, Consiglio J, Visone R, Ferracin M, Fornari F, Zanesi N, Alder H, D'Elia G, Gramantieri L, Bolondi L, Lanza G, Querzoli P, Angioni A, Croce CM, Negrini M. Oncogenic role of *miR-483-3p* at the *IGF2/483* locus. Cancer Res 2010;70:3140–9. Published OnlineFirst April 13, 2010. doi:10.1158/0008-5472.CAN-09-4456.

Lu W, Zhang G, Zhang R, Flores LG II, Huang Q, Gelovani JG, Li C. Tumor site–specific silencing of *NF-κB p65* by targeted hollow gold nanosphere–mediated photothermal transfection. Cancer Res 2010;70:3177–88. Published OnlineFirst April 13, 2010. doi:10.1158/0008-5472.CAN-09-3379.

Geng H, Rademacher BL, Pittsenbarger J, Huang C-Y, Harvey CT, Lafortune MC, Myrthue A, Garzotto M, Nelson PS, Beer TM, Qian DZ. ID1 enhances docetaxel cytotoxicity in prostate cancer cells through inhibition of p21. Cancer Res 2010;70:3239–48. Published OnlineFirst April 13, 2010. doi:10.1158/0008-5472.CAN-09-3186.

Yoo BK, Chen D, Su Z-z, Gredler R, Yoo J, Shah K, Fisher PB, Sarkar D. Molecular mechanism of chemoresistance by astrocyte elevated gene-1. Cancer Res 2010;70:3249–58. Published OnlineFirst April 13, 2010. doi:10.1158/0008-5472.CAN-09-4009.

Lu ZH, Shvartsman MB, Lee AY, Shao JM, Murray MM, Kladney RD, Fan D, Krajewski S, Chiang GG, Mills GB, Arbeit JM. Mammalian target of rapamycin activator RHEB is frequently overexpressed in human carcinomas and is critical and sufficient for skin epithelial carcinogenesis. Cancer Res 2010;70:3287–98. Published OnlineFirst April 13, 2010. doi:10.1158/0008-5472.CAN-09-3467.

Hattermann K, Held-Feindt J, Lucius R, Müerköster SS, Penfold MET, Schall TJ, Mentlein R. The chemokine receptor CXCR7 is highly expressed in human glioma cells and mediates antiapoptotic effects. Cancer Res 2010;70:3299–308. Published OnlineFirst April 13, 2010. doi:10.1158/0008-5472.CAN-09-3642.

Nadiminty N, Lou W, Sun M, Chen J, Yue J, Kung H-J, Evans CP, Zhou Q, Gao AC. Aberrant activation of the androgen receptor by NF-κB2/p52 in prostate cancer cells. Cancer Res 2010;70:3309–19. Published OnlineFirst April 13, 2010. doi:10.1158/0008-5472.CAN-09-3703.

Acu ID, Liu T, Suino-Powell K, Mooney SM, D'Assoro AB, Rowland N, Muotri AR, Correa RG, Niu Y, Kumar R, Salisbury JL. Coordination of centrosome homeostasis and DNA repair is intact in MCF-7 and disrupted in MDA-MB 231 breast cancer cells. Cancer Res 2010;70:3320–8. Published OnlineFirst April 13, 2010. doi:10.1158/0008-5472.CAN-09-3800.

McFarlane C, Kelvin AA, de la Vega M, Govender U, Scott CJ, Burrows JF, Johnston JA. The deubiquitinating enzyme USP17 is highly expressed in tumor biopsies, is cell cycle regulated, and is required for G_1-S progression. Cancer Res 2010;70:3329–39. Published OnlineFirst April 13, 2010. doi:10.1158/0008-5472.CAN-09-4152.

Dudka AA, Sweet SMM, Heath JK. Signal transducers and activators of transcription-3 binding to the fibroblast growth factor receptor is activated by receptor amplification. Cancer Res 2010;70:3391–401. Published OnlineFirst April 13, 2010. doi:10.1158/0008-5472.CAN-09-3033.

Cho SY, Xu M, Roboz J, Lu M, Mascarenhas J, Hoffman R. The effect of CXCL12 processing on $CD34^+$ cell migration in myeloproliferative neoplasms. Cancer Res 2010;70:3402–10. Published OnlineFirst April 13, 2010. doi:10.1158/0008-5472.CAN-09-3977.

Published OnlineFirst 05/11/2010.

doi: 10.1158/0008-5472.CAN-10-1347

Cancer Research
The Journal of Cancer Research (1916–1930) | The American Journal of Cancer (1931–1940)

AACR American Association for Cancer Research

Predicting Outcomes in Cervical Cancer: A Kinetic Model of Tumor Regression during Radiation Therapy

Zhibin Huang, Nina A. Mayr, William T.C. Yuh, et al.

Cancer Res 2010;70:463-470. Published OnlineFirst January 12, 2010.